



## UvA-DARE (Digital Academic Repository)

### Angiogenesis inhibition in high grade glioma

Verhoeff, J.J.C.

**Publication date**  
2009

[Link to publication](#)

#### **Citation for published version (APA):**

Verhoeff, J. J. C. (2009). *Angiogenesis inhibition in high grade glioma*. [Thesis, fully internal, Universiteit van Amsterdam].

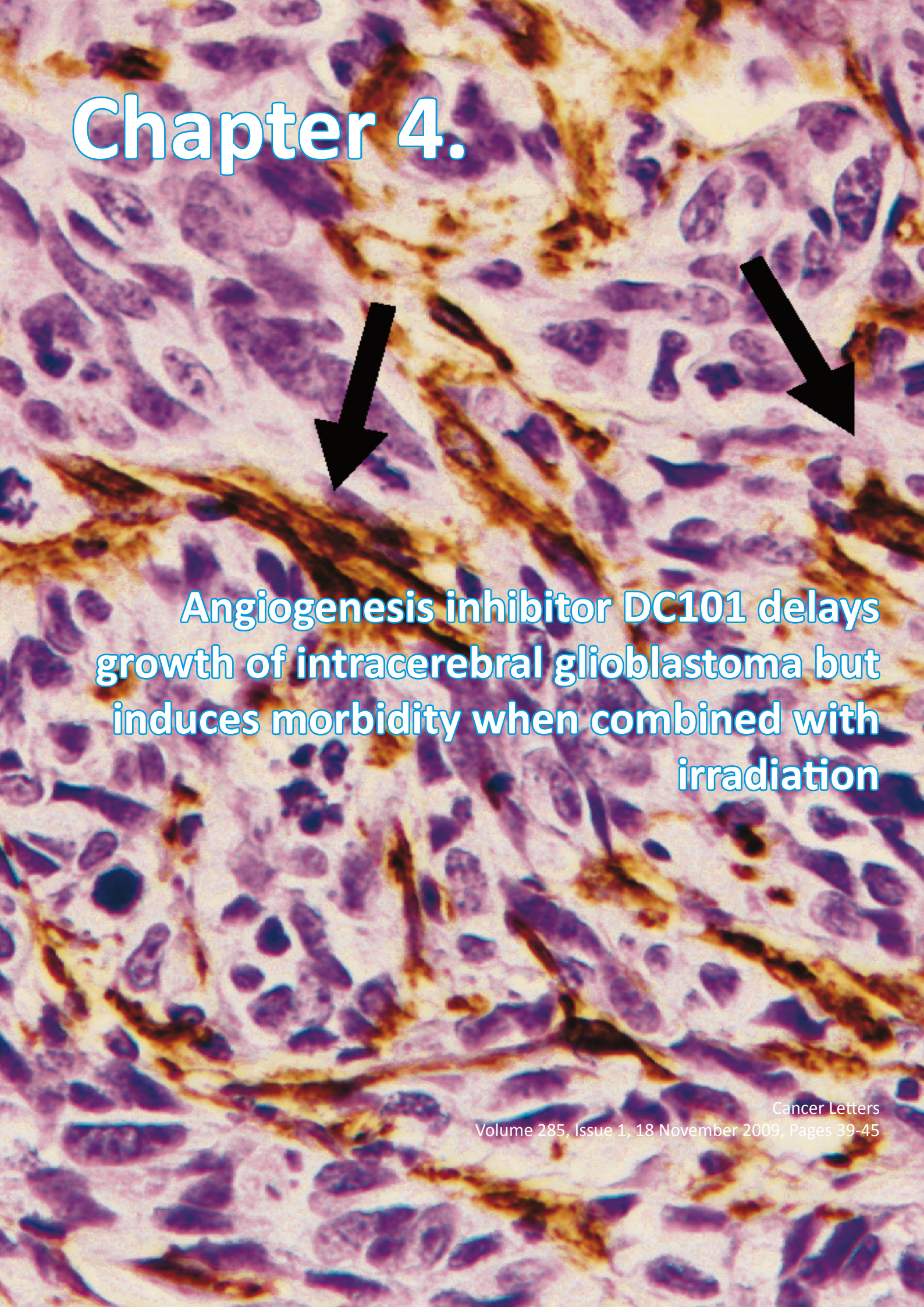
#### **General rights**

It is not permitted to download or to forward/distribute the text or part of it without the consent of the author(s) and/or copyright holder(s), other than for strictly personal, individual use, unless the work is under an open content license (like Creative Commons).

#### **Disclaimer/Complaints regulations**

If you believe that digital publication of certain material infringes any of your rights or (privacy) interests, please let the Library know, stating your reasons. In case of a legitimate complaint, the Library will make the material inaccessible and/or remove it from the website. Please Ask the Library: <https://uba.uva.nl/en/contact>, or a letter to: Library of the University of Amsterdam, Secretariat, P.O. Box 19185, 1000 GD Amsterdam, The Netherlands. You will be contacted as soon as possible.

# Chapter 4.



Angiogenesis inhibitor DC101 delays growth of intracerebral glioblastoma but induces morbidity when combined with irradiation



## Angiogenesis inhibitor DC101 delays growth of intracerebral glioblastoma but induces morbidity when combined with irradiation

Joost J.C. Verhoeff<sup>a</sup>, Lukas J.A. Stalpers<sup>a</sup>, Cornelis J.F. Van Noorden<sup>b</sup>, Dirk Troost<sup>c</sup>, Marja D. Ramkema<sup>c</sup>, Chris van Bree<sup>a</sup>, Ji-Ying Song<sup>d</sup>, Mila Donker<sup>e</sup>, Martha Chekenya<sup>f</sup>, W. Peter Vandertop<sup>e</sup>, Dick J. Richel<sup>a</sup>, Wouter R. van Furth<sup>e,\*</sup>

<sup>a</sup>Laboratory of Experimental Oncology and Radiobiology, Center for Experimental and Molecular Medicine, Academic Medical Center, University of Amsterdam, Meibergdreef 9, 1105 AZ Amsterdam, The Netherlands

<sup>b</sup>Department of Cell Biology and Histology, Academic Medical Center, University of Amsterdam, Meibergdreef 15, 1105 AZ Amsterdam, The Netherlands

<sup>c</sup>Department of Neuropathology, Academic Medical Center, University of Amsterdam, Meibergdreef 9, 1105 AZ Amsterdam, The Netherlands

<sup>d</sup>Experimental Animal Pathology, The Netherlands Cancer Institute, Plesmanlaan 121, 1066 CX Amsterdam, The Netherlands

<sup>e</sup>Department of Neurosurgery, Academic Medical Center, University of Amsterdam, Meibergdreef 9, 1105 AZ Amsterdam, The Netherlands

<sup>f</sup>Department of Biomedicine, University of Bergen, Jonas Lies vei 91, N-5009 Bergen, Norway

### ARTICLE INFO

#### Article history:

Received 3 March 2009

Received in revised form 28 April 2009

Accepted 29 April 2009

#### Keywords:

Intracranial

Glioma

Radiotherapy

Angiogenesis inhibition

Nude mouse

### ABSTRACT

The combination of irradiation with angiogenic inhibition is increasingly being investigated for treatment of glioblastoma multiforme (GBM). We investigated whether vascular endothelial growth factor receptor-2 (VEGFR-2) inhibitor DC101 affects morbidity and tumor growth in irradiated and non-irradiated intracerebral GBM-bearing mice, controlled with sham treatments. End-points were toxicity, morbidity and histology. Irradiation either or not combined, reduced tumor size strongly, whereas DC101 mono-treatment reduced tumor size by 64%. Irradiation delayed morbidity from 5.8 weeks in sham-treated mice to 10.3 weeks. Morbidity after combined treatment occurred after 5.9 weeks. Treatment with angiogenesis inhibitor DC101 delays tumor growth but it induces morbidity, by itself or combined with irradiation.

© 2009 Elsevier Ireland Ltd. All rights reserved.

### 1. Introduction

Glioblastoma multiforme (GBM) accounts for approximately one third of all intracranial tumors and is one of the most aggressive brain tumors. Conventional treatment of GBM consists of surgical resection followed by radiotherapy and chemotherapy. Despite this intense treatment, tumors invariably recur, usually arising within 2 cm of the original resection margin [1].

The mechanisms of the high radioresistance of GBM are largely unknown, but the vascular system is considered to play a key role in radiation response, tumor growth and

invasion [2,3]. Vascular endothelial growth factor (VEGF) is the best-characterized and likely the most potent angiogenic factor. VEGF increases vascular permeability and stimulates vessel formation by recruiting progenitor endothelial cells [4,5]. Systemic therapy directed against the VEGF pathway improves the response to focal irradiation of a subcutaneous GBM tumor in a mouse model [6]. However, location of the tumor, subcutaneous in the flank versus intracranial, affects irradiation effects on gene expression in the tumor [7]. The microenvironment and tumor location have impact on tumor growth, tumoral vessel formation, metastasis and therapy [8–11]. Endothelial cells in GBM tumors also show different gene expression patterns depending on the location of the tumors in the body [12]. Therefore, an orthotopic GBM tumor model is considered to be clinically more relevant.

\* Corresponding author. Tel.: +31 2056691111; fax: +31 206091278.  
E-mail address: [w.r.vanfurth@amc.uva.nl](mailto:w.r.vanfurth@amc.uva.nl) (W.R. van Furth).

Since angiogenesis inhibitors are thought to normalize tumor vessels resulting in improved blood flow and oxygenation [13], the combination of angiogenesis inhibition with irradiation might potentiate the cell kill and sensitize effects of irradiation [14]. First clinical trials show a safe and feasible use of combined irradiation and angiogenic inhibition, although toxicities (e.g. intratumoral hemorrhage, wound dehiscence, and bowel perforation) and patterns of relapse (e.g. satellite formation) need to be monitored closely [15,16]. High-dose irradiation of the mouse brain is restricted by acute irradiation toxicity to the esophagus and trachea [17]. Therefore, single fraction or low-dose short-term treatments are usually given [6,18–22]. To circumvent toxicity we developed an intracranial irradiation model using superficially-implanted low-active iodine-125 brachytherapy seeds, that allows clinically relevant radiotherapy of the murine brain, without side effects [17]. First a guide-screw with a central canal was implanted intracranially, 3 weeks later human glioma cells were administered through the canal of the guide-screw and 1 week later tightly fitting radioactive or sham seeds were inserted. In the present study, we investigated the effects of treatment with the vascular endothelial growth factor receptor-2 (VEGFR-2) blocker DC101, by itself or in combination with irradiation, on tumor growth and morbidity in this orthotopic GBM mouse model with intracranial irradiation. Morbidity was defined as at least 20% weight loss and/or signs of neurological pathology.

## 2. Materials and methods

### 2.1. Cell line

The human derived GBM cell line U251-NG2 was selected for the present study. It is a transfected U251 cell line which overexpresses glial precursor proteoglycan NG2, showing an invasive, highly-vascular growth pattern in the rat brain [23,24]. We selected this cell line for the present study because U251-NG2 tumors reflect as closely as possible clinically relevant GBM growth and treatment response. The cell line is not overly radiosensitive and does not depend too strongly on the VEGF pathway [25]. The high vascularization of U251-NG2 tumors is considered to be the result of diminished inhibition of angiogenesis [23]. In addition, it has the typical mutational status of many GBMs (p53 and PTEN) [26]. VEGF expression levels are not different from other GBM cell lines that are not genetically modified. The U251-NG2 cell line was xenotransplanted into the nude mouse brain. Cells were cultured and transplanted as described previously [17].

### 2.2. Orthotopic murine model

Athymic Nude-*nu* female mice (Harlan, Horst, The Netherlands), 4–6 weeks of age, were kept under specific pathogen-free conditions with optimal feeding, temperature, hygienic conditions and ample space, according to stringent experimental animal facility regulations. Orthotopic gliomas were xenografted as previously described [17]. In short, on day 0, therapy was started. On day –28,

we implanted a hollow guide-screw into the skulls of the mice. On day –7, we slowly injected  $5 \times 10^5$  cancer cells in 3  $\mu$ l PBS into the right frontolateral brain, 2 mm below the screw. We hypothesized to find an additive treatment effect on tumor growth delay of at least 30%. With a power of 80% and a predicted standard deviation of 3 days, group size should be seven mice or more. Two separate but identical experiments were performed on cohorts of 43 and 41 mice, respectively. All murine experiments were approved, monitored and reviewed by the university committee on animal experiments. Seven of 91 mice (7.7%) died during surgical procedures and were thus excluded from the study.

### 2.3. Treatment regimens

Over 13 weeks, concurrent cranial irradiation with 2 mCi iodine-125 ( $^{125}\text{I}$ , Model 6711; Medi-Physics; Amersham, Arlington Heights, IL) delivered a minimal tumor dose of 23.0 Gy at 5 mm below the seed (Bio Equivalent Dose<sub>tumor</sub> (BED<sub>tumor</sub>) = 30.6 Gy), 52.1 Gy at 2.5 mm below the seed, and 6.8 Gy at 10 mm below the seed, the ‘pharynx dose’ [17]. We inserted the  $^{125}\text{I}$  seed on day 0 through the hollow screw as described before (Fig. 1). The  $^{125}\text{I}$  concurrent cranial irradiation model enabled local high-dose irradiation whereby fatal irradiation toxicity as observed in other cranial radiation modalities was prevented. Randomly-selected mice received  $^{125}\text{I}$  seeds; the others received inactive seeds as sham treatment.

Anti-angiogenesis treatment was started directly after seed insertion on day 0. The rat anti-mouse VEGFR-2 antibody (DC101) actively prevents tumor growth when applied every 3 days in dosages of 40 mg/kg or higher [27]. DC101 was administered intraperitoneally in doses of 40 mg/kg every 3 days, a schedule with biological activity and low toxicity profile [6,27–29]. Both treatment modalities, irradiation and angiogenesis pathway inhibition, were

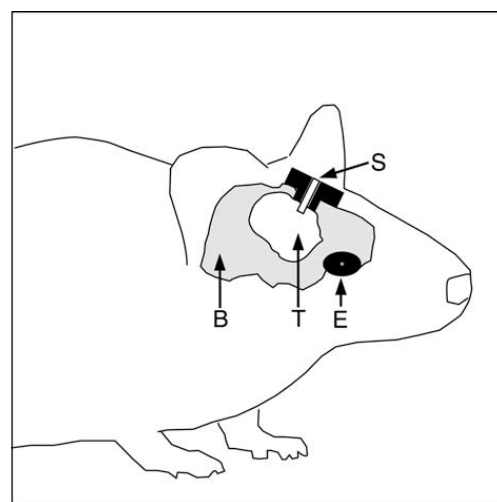


**Fig. 1.** Schematic sagittal view through the head of an intracerebral brain tumor-bearing mouse with implanted screw containing an  $^{125}\text{I}$  brachytherapy seed. Cumulative minimal radiation dose on the tumor during 13 weeks at 5 mm below the 2 mCi  $^{125}\text{I}$  brachytherapy seed is 23.0 Gy (integrated BED 30.6 Gy). B, brain; E, eye; S, subcutaneous plastic guide-screw through the skull; T, tumor (adapted from [17]).

controlled with sham treatments, resulting in 4 treatment regimen groups. Regimen 1 (R1;  $n = 20$ ) consisted of sham radiation treatment and injections of PBS (similar volumes as DC101 injections); regimen 2 (R2;  $n = 21$ ) combined sham radiation treatment and DC101 therapy; regimen 3 (R3;  $n = 21$ ) combined  $^{125}\text{I}$  radiotherapy and injections of PBS; regimen 4 (R4;  $n = 22$ ) consisted of irradiation and DC101 injections.

After a maximum of 13 weeks of treatment, all surviving mice were sacrificed by  $\text{CO}_2$  asphyxiation in a sealed cage and brains were dissected for histological analysis. Animals were sacrificed earlier when signs of morbidity occurred such as weight loss exceeding 20%. Physical or neurological signs were scored daily and were also cues for euthanasia. Specific signs were posture changes, diminished activity, diminished turgor, rotational behavior or a domehead – a phenomenon of skull expansion by extreme tumor growth. Brains were fixed and kept in formaldehyde until used. All brains were coded randomly.

#### 2.4. Histological and immunohistochemical analysis

Histological analysis was performed on blindly coded material. Formaldehyde-fixed, paraffin-embedded tissue blocks were sectioned axially in their entirety (section thickness,  $8\ \mu\text{m}$ ) for histological and immunohistochemical analysis. Each 20th axial section was stained with hematoxylin–eosin. The section with the maximum cross sectional size of the tumor was used to calculate percentage tumor area as  $\frac{\text{tumor area}}{\text{total brain area}} * 100$ .

Additional analysis was performed on axial sections immediately following the one with the largest tumor area, for all mice in the second experiment ( $n = 41$ ). These sections were also evaluated blindly. Nissl-stained sections (Cresylechtviolet; Sigma–Aldrich, Zwijndrecht, The Netherlands) were used to count mitotic figures present in three randomized high power fields (hpfs) to establish the Nissl mitosis index. Tumor cell proliferation index was established by counting the cells with positive nuclei after staining with an antibody against KI-67 antigen (MIB-1; Dako, Glostrup, Denmark) in three randomized hpfs. The apoptosis index was determined by counting apoptotic cells in three randomized hpfs of sections stained with an anti-cleaved caspase 3 antibody (Cell Signaling Technology, Danvers, MA). Necrosis in the tumor area was scored semiquantitatively in Nissl-stained sections using the grading 'none (0), minimal (1), present (2) and extensive (3)'. An index of reactive gliosis (a neuroinflammatory response around the tumor with neuropathological consequences) was determined in sections stained with an anti-gial fibrillary acidic protein (GFAP) antibody (Dako) and scored semiquantitatively using the grading 'none (0), minimal (1), present (2) and extensive (3)'.

Satellite tumors at a distance  $>200\ \mu\text{m}$  from the original tumor were counted in the sections with the largest tumor area. CD34 is expressed on freshly recruited endothelial progenitor cells that respond to tumor angiogenesis signals [30]. When any CD34-positive endothelial cells were found in structured tumor blood vessels in sections with the largest tumor area, the tumor was considered CD34-positive (anti-mouse CD34; Cedarlane, Burlington, Canada). Pres-

ence of any  $\alpha$ -smooth muscle actin (SMA)-positive cells in sections with the largest tumor area was considered to be a hallmark of vessel maturation (monoclonal anti-mouse  $\alpha$ -SMA; Dako) [31].

#### 2.5. Mouse pathology

Ten mice bearing intracranial tumors and four mice without tumors receiving combined treatment were subjected to pathologic analysis. After 17 days, four randomly-selected mice were euthanized to analyze short term effects of the combined treatment. One of these four mice did not receive a tumor prior to start of therapies. After 6 weeks of treatment, all remaining mice were sacrificed and all major organs such as the gastrointestinal tract, liver, kidney, pancreas, kidneys, heart, lung, lymph nodes, bone marrows as well as organs in the head and neck region were sampled and microscopically examined. The time points for sacrifice were selected on the basis of morbidity curves. Furthermore, we administered DC101 for 13 weeks to five non-tumor-bearing mice, confirming previously reported safety of the drug as mono-treatment in this dosage.

#### 2.6. Data analysis

Differences in tumor volume, index of mitosis, proliferation, apoptosis, necrosis, reactive gliosis, number of satellites, vessel density, relative weight loss and survival were analyzed using the unpaired  $t$ -test for equality of means when data were distributed normally or the Mann–Whitney rank-sum test when data were not distributed normally, using SPSS® software (SPSS, Chicago, IL). Kaplan–Meier survival analysis was performed on the survival data. Differences were considered significant when  $p \leq 0.05$ .

### 3. Results

#### 3.1. Survival and morbidity

Signs of morbidity of mice in the four treatment groups are shown in Table 1. In both groups receiving DC101 (R2 and R4), approximately 75% of the mice lost more than 20% weight in the 13 weeks of treatment. Espe-

**Table 1**

Physical signs and cues of morbidity in mice bearing intracranial glioma that were sham treated (Sham), DC101 treated (DC101), irradiated (Irrad) or both DC101 treated and irradiated (Comb).

Signs of morbidity	Sham	DC101	Irrad	Comb
	( $n = 20$ )	( $n = 21$ )	( $n = 21$ )	( $n = 22$ )
Weight loss exceeding 20%	10	15	5	16
Postural change	6	4	4	12
Decreased activity	6	5	5	7
Domehead	7	3	1	3
Reduced turgor	1	2	0	7
Rotational behavior	1	1	3	2
Lethal bowel edema	0	1	0	1
Total pre-term sacrificed (<13 weeks)	19	19	7	19
Sacrificed at end of study (at 13 weeks)	1	2	14	3
Mean survival (weeks)	5.8	5.2	10.3	5.9

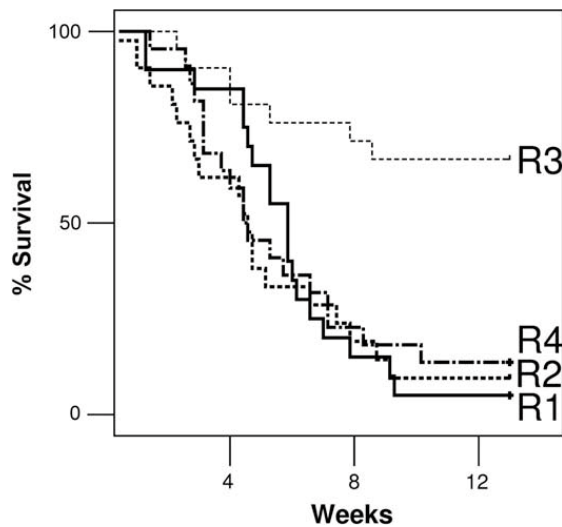


**Fig. 2.** Kaplan-Meier curves of survival in weeks for nude mice that were inoculated intracranially with U251-NG2 GBM cancer cells and subsequently sham treated (R1), DC101 treated (R2), irradiated (R3) or both DC101 treated and irradiated (R4). Log rank  $p < 0.01$  of R1 versus R2, R3 and R4.

cially mice that received both DC101 and irradiation (R4) showed weight loss accompanied by posture changes, decreased activity and reduced tumor. Mean relative end weight of the sham-treated mice was 89.2% versus 78.5% in the DC101 group ( $p < 0.02$ ). Mean relative end weight in the irradiation group was 91.2% versus 78.3% in the combined treated group ( $p < 0.01$ ).

Fig. 2 shows Kaplan-Meier survival curves determined for the four groups of mice. Mean survival of sham-treated mice (R1) was 5.8 weeks only. Administration of DC101 alone (R2) did not improve survival (mean 5.2 weeks;  $p = 0.53$ ). Irradiation treatment alone (R3) delayed occurrence of mouse morbidity by 4.5 weeks to a mean of 10.3 weeks ( $p < 0.002$ ). However, combined treatment of irradiation with DC101 (R4) yielded an unexpected poor survival outcome of 5.9 weeks only, similar to that of sham treatment.

3.2. Tumor development

Figs. 3 and 4 summarize the results of histological examination of tumors and brains.

Sham-treated mice (R1) had, as expected, the largest tumors irrespective of the time of sacrifice, covering on average 44% of the surface of the largest cross section through the brain (Fig. 3A). These sham-treated control tumors had the highest proliferation index (88.6%; Fig. 3B) and highest numbers of mitotic cells (Fig. 3C). Reactive gliosis was qualified as ‘extensive’ in the untreated group (R1) (Fig. 3F).

DC101-treated mice (R2) had significantly smaller tumors, with a size reduction of 64% compared to untreated tumors (Fig. 3A). DC101 treatment did not reduce cell proliferation significantly ( $p < 0.07$ ), but mitosis was significantly reduced. All other tumor parameters were not different in sham-treated and DC101-treated mice (Fig. 3B–H).

Irradiated mice (R3) had no detectable tumors in 13 of 21 cases (62%), or they were greatly reduced in size as compared to untreated animals (Fig. 3A). In the tumors that were present, all parameters were significantly reduced in number or score, except necrosis score which was similar (Fig. 3B–H). Large areas around the injection site were necrotic due to irradiation while few apoptotic cells were present at the moment of analysis, indicating that the anti-tumor effect already occurred at an earlier time point.

Combined irradiation with DC101 treatment (R4) yielded almost complete local tumor control with a mean tumor size of 0.1%, compared to tumors of sham-treated mice (Fig. 3A). All parameters were reduced or absent in the tumors except for the necrosis score (Fig. 3B–H).

3.3. Mouse pathology

Post-mortem examination was performed on four animals that received combined treatment for 17 days and on 10 animals that received combined treatment for 6 weeks (Table S1). This revealed pathology mainly of the peritoneal cavity, namely the intestinal tract and pancreas that showed edematous changes. We found more edematous changes in mice sacrificed at the latter time point. About one third of all animals analyzed had ascites. Also observed, but with much lower frequency, were other lesions such as angitis in the lungs, arteritis in the lamina muscularis of the small intestine, colitis, ileitis, jejunitis, duodenitis, peritonitis, angiomatous changes of the mesenteric lymph nodes, and interstitial pneumonia. Organs in the head and neck region were not affected seriously, although in some cases inflammatory lesions in the nasal cavity

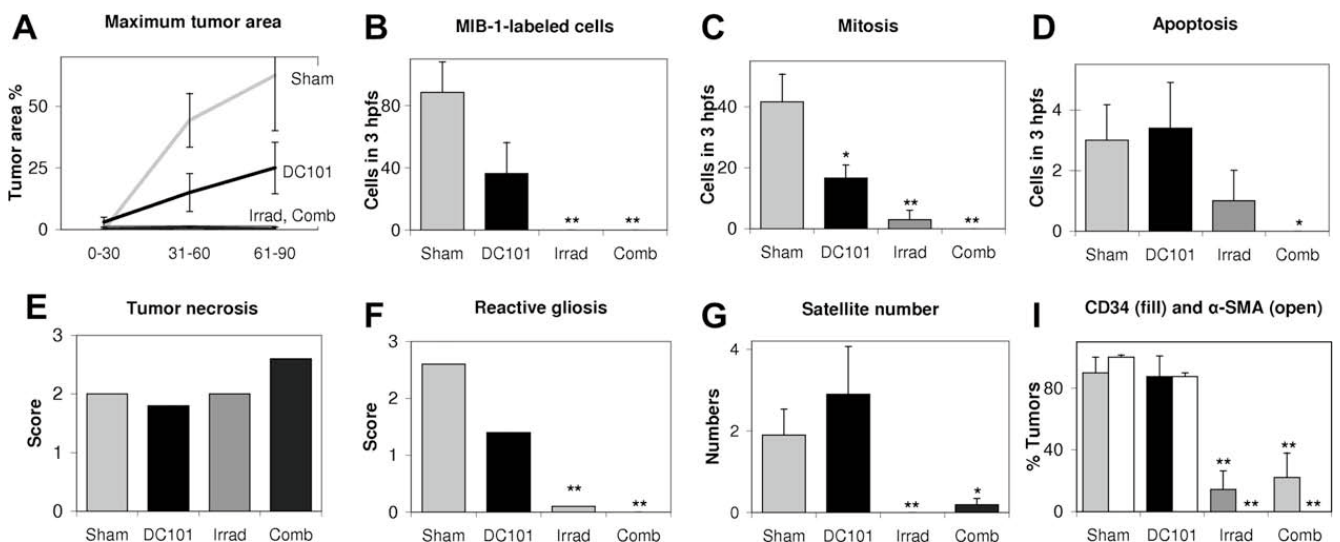


**Fig. 3.** Characteristics of GBM from sham-controlled mice (light grey bars), DC101-treated mice (dark black bars), irradiated mice (dark grey bars) and mice treated with the combined regimen (light black bars). Error bars indicate SEM; \* $p < 0.05$ , \*\* $p < 0.02$  compared to sham treatment: (A) mean maximum tumor area. Mice were pooled in three groups that survived 0–30 days, 31–60 days and 61–90 days, respectively. Tumors of irradiated mice and mice treated with combined regimen were very small; (B) MIB-1-labeled nuclei indicating proliferative cells in tumors; (C) mitotic cells in tumors; (D) apoptotic cells in tumors; (E) necrosis in the tumor area scored as none (0), minimal (1), present (2) or extensive (3); (F) reactive gliosis, a neuroinflammatory response around the tumor with neuropathological consequences, scored in the same way as under E; (G) tumor satellites surrounding the main tumor mass at a distance  $>200 \mu\text{m}$  and (H) mean percentage of tumors with CD34- and  $\alpha$ -SMA-positive intratumoral microvessels.

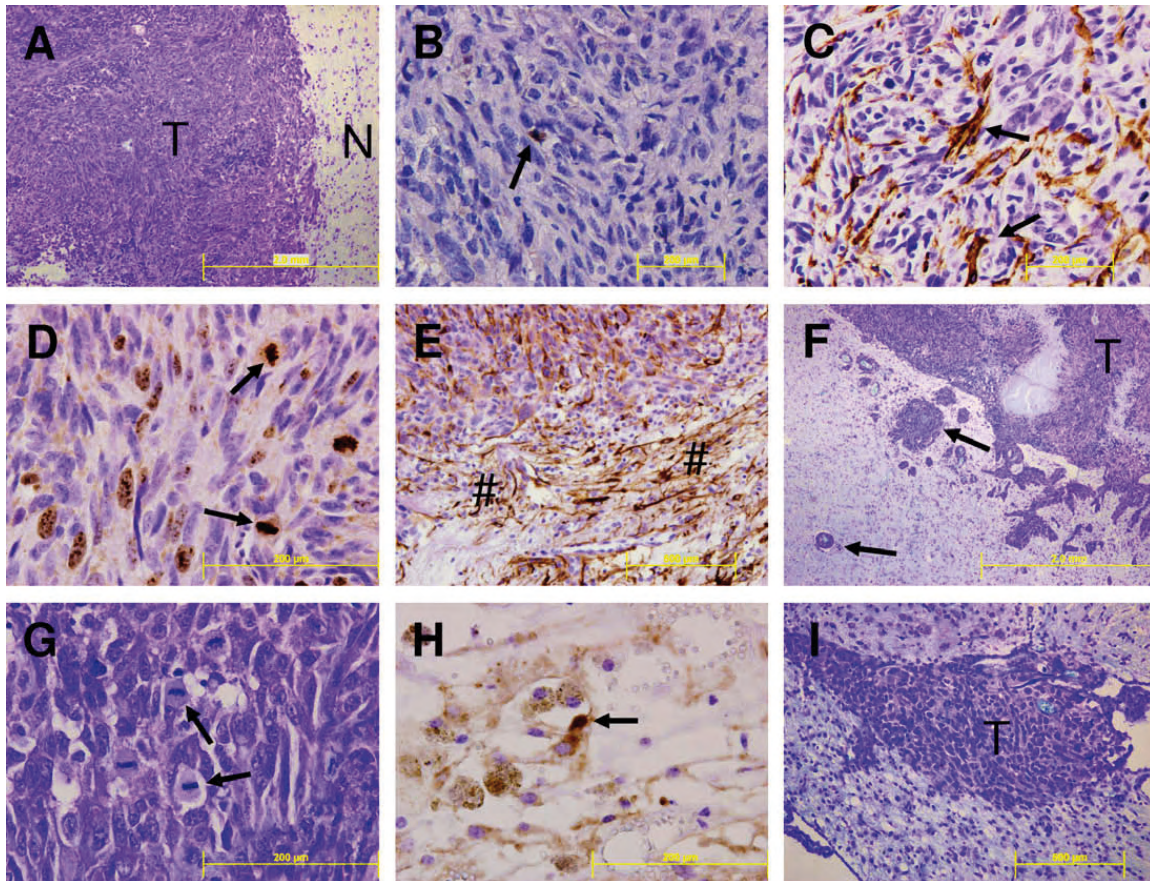


**Fig. 4.** H&E-stained (A, F, G and I) and immunohistologically-stained (B, C, D, E and H) sections of brain of nude mice inoculated with U251-NG2 GBM cells after 13 weeks of treatment. A, B, C, D and E: sham-treated animals; F and G: DC101 treated animals; H: Irradiated animals; I: Combined treatment with irradiation and DC101. (A) H&E-stained large tumor load (T) surrounded by normal brain tissue (N). (B) Anti-active caspase 3 staining showing an apoptotic cell (arrow). (C) SMA-positive vessels (arrows). (D) MIB-1-labeled nuclei (arrows), (E) Reactive gliosis (#). (F) Invading tumor satellites (arrows). (G) Mitotic cancer cells (arrows). (H) Apoptotic cancer cells (arrows) in anti-active caspase 3 staining. (I) Largest tumor (T) in R4 group of mice. Bars, A, D, F: 2.0 mm, B, C, G, H: 0.2 mm, E, I: 0.5 mm.

were observed. In one animal, severe lesions of lymphoma were encountered, which were probably background pathology. There was no correlation between severity of weight loss and severity of pathology. Non-tumor-bearing mice demonstrated the same pathological findings as tumor-bearing mice. DC101 therapy for 13 weeks in non-tumor-bearing mice did not induce weight loss, but these mice did not gain weight as sham-treated mice did.

#### 4. Discussion

We investigated the effects of concurrent cranial irradiation combined with systemic angiogenesis inhibition by VEGFR-2 blockade on tumor growth and morbidity of intracranial GBM-bearing nude mice. The major advantage of our orthotopic brain tumor model is the similarity with the clinical situation [17]. As expected, sham-treated mice showed highly proliferative, large tumors. DC101 treatment significantly reduced tumor size, but morbidity did not improve. Irradiation induced tumor growth delay and reduced morbidity significantly. Combinational treatment improved local tumor control but, surprisingly, morbidity and survival were comparable to that of sham-treated animals.

Winkler et al. combined external beam irradiation with DC101 treatment in an orthotopic GBM model [20]. The authors observed synergistic effects on morphology and

function of tumor vessels during a normalization window, between day 5 and day 8 of treatment but did not describe effects of treatment on morbidity as we did in our study. Systemic toxicity of combined DC101 and irradiation in mice was not anticipated, as it was never reported before, although bowel toxicity has been described as a prominent inadvertent effect of VEGF inhibitors in clinical studies [32–35]. We also found in mice that combined treatment mainly caused pathology of the gastrointestinal tract. We did not observe the esophageal damage that was expected after irradiation treatment in the head and neck region. When comparing DC101 mono-treatment with the combined treatment morbidity profile, we more often found postural changes and more often scored reduced turgor in the combined treatment group. This indicates that extracranial side effects caused the higher toxicity. The fact that local irradiation to the brain appears to exacerbate DC101 toxicity is of great concern.

In our present study, irradiation alone and DC101 treatment alone were well-tolerated, but DC101 treatment alone showed similar morbidity as sham treatment. Kozin et al. [6] found that 40 mg/kg DC101 with whole body irradiation was well-tolerated by mice implanted with U87 GBM cancer cells in the flank. On the other hand, these authors found that the same dose of DC101 was poorly tol-

erated by mice with heterotopically-implanted 54A small cell lung carcinoma cells; 44% of the mice died from unsuspected intestinal toxicity. This difference was explained by assuming that VEGFR-2 inhibitor DC101 was absorbed by the U87 tumors and not by the 54A tumors. The latter, i.e. no sequestering of DC101 by the tumor, could be the case for U251-NG2 tumors as well because of its more clinically comparable VEGF production [25]. Nevertheless, non-tumor-bearing mice demonstrated comparable pathologic findings.

Not only selection of cancer cell line but also sequence of treatments are important factors for outcome of combined anti-angiogenesis and irradiation treatment. Williams et al. [36] showed in a non-small-cell lung carcinoma mouse model that concurrent ZD6474 anti-angiogenic treatment produces some enhancement of fractionated radiotherapy whereas sequential administration leads to a highly significant interaction between ZD6474 treatment and irradiation. Ning et al. [37] showed also that radioenhancement was greater when the anti-angiogenic SU5416 was administered after each radiation dose instead of prior to radiation. Abrogation of VEGF-dependent survival signaling in endothelial cells may be the mechanistic basis for the enhancing effect of ZD6474 treatment on radiotherapy in a sequential schedule [36]. We employed a concurrent schedule of irradiation and DC101 treatment and discovered that side effects overshadowed potential anti-tumor benefits. This important finding should be taken into account in the design of clinical studies.

A blockade of VEGFR-2 leads to increased levels of VEGF in the circulation of mice and humans [27,38]. Not only VEGF levels are increased, but also signaling through VEGFR-3 may be enhanced when VEGFR-2 is blocked [39]. This pathway is involved in lymph-angiogenesis and may explain lymph edema and edema of submucosa of the intestines that probably causes the observed morbidity.

Resection material from five patients before and after treatment with bevacizumab revealed a trend toward a relative increase of CD34 and  $\alpha$ -SMA immunostaining following treatment [40]. Where others found also functional effects of treatment with DC101, we did not detect significant effects on tumor vasculature as assessed with CD34 and  $\alpha$ -SMA staining after long term treatment, which is surprising: an anti-angiogenic agent that inhibits VEGFR-2 has apparently no long term effect on vessel composition. Less toxic lower dosages of DC101 are therefore presumably not clinically relevant. On the other hand, there was an anti-angiogenic effect, because DC101 did affect tumor growth in our experiment by decreasing proliferation. It is quite possible that vascular density remained the same, in the face of an anti-angiogenic effect that slows tumor growth. In addition to this, as suggested in recent publications, VEGF inhibition by DC101 probably induces normalization of blood flow in aberrant tumor vasculature rather than a true pruning effect [20]. Although formation of tumor satellites was not significantly affected in this experiment, it is an important side effect of anti-angiogenic treatment, caused by cooption of pre-existent vessels [41,42]. Interestingly, diffusely invading glioma cells did not respond to monotherapy with DC101 in vivo [43]. Anti-angiogenic treatment is effective against solid compo-

nents of GBM but is largely ineffective against the invasive, angiogenesis-independent tumor component. The tumor model in our study probably reflected the former more than the latter. It may be the Achilles' heel of anti-VEGF treatment as mono-therapy in the clinical setting.

Further studies are needed with other VEGF inhibitors to analyze safety and efficacy of these compounds when combined with irradiation to support clinical implementation. Although trialed for one inhibitor in the standard dose, our findings are an important warning for pre-clinical and clinical trials aimed at combining radiotherapy and apparently harmless angiogenesis inhibitors, as is also reported in clinical studies [34]. The combination of radiotherapy with VEGFR-2 blockade can potentiate tumor growth delay but may inadvertently lead to unexpected morbidity.

## 5. Conflict of interest

Actual or potential conflicts of interest do not exist.

## Acknowledgements

The authors thank Dr. D.J. Hicklin and Dr. Z. Zhu (ImClone Systems, New York, NY) for the generous provision of DC101; Dr. J. Haveman and Dr. M.R. Sprick for discussion and advice; and Dr. K. Koedooder for assistance with the iodine-125 seeds.

## Appendix A. Supplementary material

Supplementary data associated with this article can be found, in the online version, at doi:10.1016/j.canlet.2009.04.038.

## References

- [1] F.H. Hochberg, A. Pruitt, Assumptions in the radiotherapy of glioblastoma, *Neurology* 30 (1980) 907–911.
- [2] N. Ferrara, T. Davis-Smyth, The biology of vascular endothelial growth factor, *Endocr. Rev.* 18 (1997) 4–25.
- [3] J. Holash, S.J. Wiegand, G.D. Yancopoulos, New model of tumor angiogenesis: dynamic balance between vessel regression and growth mediated by angiopoietins and VEGF, *Oncogene* 18 (1999) 5356–5362.
- [4] M. Toi, T. Matsumoto, H. Bando, Vascular endothelial growth factor: its prognostic, predictive, and therapeutic implications, *Lancet Oncol.* 2 (2001) 667–673.
- [5] Y. Shaked, A. Ciarrocchi, M. Franco, C.R. Lee, S. Man, A.M. Cheung, D.J. Hicklin, D. Chaplin, F.S. Foster, R. Benezra, R.S. Kerbel, Therapy-induced acute recruitment of circulating endothelial progenitor cells to tumors, *Science* 313 (2006) 1785–1787.
- [6] S.V. Kozin, Y. Boucher, D.J. Hicklin, P. Bohlen, R.K. Jain, H.D. Suit, Vascular endothelial growth factor receptor-2-blocking antibody potentiates radiation-induced long-term control of human tumor xenografts, *Cancer Res.* 61 (2001) 39–44.
- [7] K. Camphausen, B. Purow, M. Sproull, T. Scott, T. Ozawa, D.F. Deen, P.J. Tofilon, Orthotopic growth of human glioma cells quantitatively and qualitatively influences radiation-induced changes in gene expression, *Cancer Res.* 65 (2005) 10389–10393.
- [8] T.J. MacDonald, T. Taga, H. Shimada, P. Tabrizi, B.V. Zlokovic, D.A. Cheresh, W.E. Laug, Preferential susceptibility of brain tumors to the antiangiogenic effects of an  $\alpha(v)$  integrin antagonist, *Neurosurgery* 48 (2001) 151–157.
- [9] L. Taillandier, L. Antunes, K.S. Angioi-Duprez, Models for neuro-oncological preclinical studies: solid orthotopic and heterotopic grafts of human gliomas into nude mice, *J. Neurosci. Methods* 125 (2003) 147–157.

- [10] B. Blouw, H. Song, T. Tihan, J. Bosze, N. Ferrara, H.P. Gerber, R.S. Johnson, G. Bergers, The hypoxic response of tumors is dependent on their microenvironment, *Cancer Cell* 4 (2003) 133–146.
- [11] E.I. Fomchenko, E.C. Holland, Mouse models of brain tumors and their applications in preclinical trials, *Clin. Cancer Res.* 12 (2006) 5288–5297.
- [12] C. Charalambous, F.M. Hofman, T.C. Chen, Functional and phenotypic differences between glioblastoma multiforme-derived and normal human brain endothelial cells, *J. Neurosurg.* 102 (2005) 699–705.
- [13] R.K. Jain, Normalization of tumor vasculature: an emerging concept in antiangiogenic therapy, *Science* 307 (2005) 58–62.
- [14] C. Nieder, N. Wiedenmann, N. Andratschke, M. Molls, Current status of angiogenesis inhibitors combined with radiation therapy, *Cancer Treat. Rev.* 32 (2006) 348–364.
- [15] P.H. Gutin, F.M. Iwamoto, K. Beal, N.A. Mohile, S. Karimi, B.L. Hou, S. Lymberis, Y. Yamada, J. Chang, L.E. Abrey, Safety and efficacy of bevacizumab with hypofractionated stereotactic irradiation for recurrent malignant gliomas, *Int. J. Radiat. Oncol. Biol. Phys.* (2009).
- [16] A. Narayana, P. Kelly, J. Golfinos, E. Parker, G. Johnson, E. Knopp, D. Zagzag, I. Fischer, S. Raza, P. Medabalmi, P. Eagan, M.L. Gruber, Antiangiogenic therapy using bevacizumab in recurrent high-grade glioma: impact on local control and patient survival, *J. Neurosurg.* 110 (2009) 173–180.
- [17] J.J. Verhoeff, L.J. Stalpers, A.W. Coumou, K. Koedooder, C. Lavini, C.J. Van Noorden, J. Haveman, W.P. Vandertop, W.R. van Furth, Experimental iodine-125 seed irradiation of intracerebral brain tumors in nude mice, *Radiat. Oncol.* 2 (2007) 38.
- [18] E.L. Lund, L. Bastholm, P.E. Kristjansen, Therapeutic synergy of TNP-470 and ionizing radiation: effects on tumor growth, vessel morphology, and angiogenesis in human glioblastoma multiforme xenografts, *Clin. Cancer Res.* 6 (2000) 971–978.
- [19] C. Hess, V. Vuong, I. Hegyi, O. Riesterer, J. Wood, D. Fabbro, C. Glanzmann, S. Bodis, M. Pruschy, Effect of VEGF receptor inhibitor PTK787/ZK222584 [correction of ZK222548] combined with ionizing radiation on endothelial cells and tumour growth, *Br. J. Cancer* 85 (2001) 2010–2016.
- [20] F. Winkler, S.V. Kozin, R.T. Tong, S.S. Chae, M.F. Booth, I. Garkavtsev, L. Xu, D.J. Hicklin, D. Fukumura, E. di Tomaso, L.L. Munn, R.K. Jain, Kinetics of vascular normalization by VEGFR2 blockade governs brain tumor response to radiation: role of oxygenation, angiopoietin-1, and matrix metalloproteinases, *Cancer Cell* 6 (2004) 553–563.
- [21] J.N. Sarkaria, B.L. Carlson, M.A. Schroeder, P. Grogan, P.D. Brown, C. Giannini, K.V. Ballman, G.J. Kitange, A. Guha, A. Pandita, C.D. James, Use of an orthotopic xenograft model for assessing the effect of epidermal growth factor receptor amplification on glioblastoma radiation response, *Clin. Cancer Res.* 12 (2006) 2264–2271.
- [22] G. Tabatabai, B. Frank, A. Wick, D. Lemke, G. von Kurthy, U. Obermuller, S. Heckl, G. Christ, M. Weller, W. Wick, Synergistic anti-glioma activity of radiotherapy and enzastaurin, *Ann. Neurol.* 61 (2007) 153–161.
- [23] M. Chekenya, M. Hjelstuen, P.O. Enger, F. Thorsen, A.L. Jacob, B. Probst, O. Haraldseth, G. Pilkington, A. Butt, J.M. Levine, R. Bjerkvig, NG2 proteoglycan promotes angiogenesis-dependent tumor growth in CNS by sequestering angiostatin, *FASEB J.* 16 (2002) 586–588.
- [24] C. Brekke, A. Lundervold, P.O. Enger, C. Brekken, E. Stalsett, T.B. Pedersen, O. Haraldseth, P.G. Kruger, R. Bjerkvig, M. Chekenya, NG2 expression regulates vascular morphology and function in human brain tumours, *Neuroimage* 29 (2006) 965–976.
- [25] K.E. Hovinga, L.J. Stalpers, C. van Bree, M. Donker, J.J. Verhoeff, H.M. Rodermond, D.A. Bosch, W.R. van Furth, Radiation-enhanced vascular endothelial growth factor (VEGF) secretion in glioblastoma multiforme cell lines – a clue to radioresistance?, *J. Neurooncol.* 74 (2005) 99–103.
- [26] M. Chekenya, C. Krakstad, A. Svendsen, I.A. Netland, V. Staalesen, B.B. Tysnes, F. Selheim, J. Wang, P.O. Sakariassen, T. Sandal, P.E. Lonning, T. Flatmark, P.O. Enger, R. Bjerkvig, M. Sioud, W.B. Stallcup, The progenitor cell marker NG2/MPG promotes chemoresistance by activation of integrin-dependent PI3K/Akt signaling, *Oncogene* 27 (2008) 5182–5194.
- [27] G. Bocci, S. Man, S.K. Green, G. Francia, J.M. Ebos, J.M. du Manoir, A. Weinerman, U. Emmenegger, L. Ma, P. Thorpe, A. Davidoff, J. Huber, D.J. Hicklin, R.S. Kerbel, Increased plasma vascular endothelial growth factor (VEGF) as a surrogate marker for optimal therapeutic dosing of VEGF receptor-2 monoclonal antibodies, *Cancer Res.* 64 (2004) 6616–6625.
- [28] P. Kunkel, U. Ulbricht, P. Bohlen, M.A. Brockmann, R. Fillbrandt, D. Stavrou, M. Westphal, K. Lamszus, Inhibition of glioma angiogenesis and growth in vivo by systemic treatment with a monoclonal antibody against vascular endothelial growth factor receptor-2, *Cancer Res.* 61 (2001) 6624–6628.
- [29] K. Lamszus, M.A. Brockmann, C. Eckerich, P. Bohlen, C. May, U. Mangold, R. Fillbrandt, M. Westphal, Inhibition of glioblastoma angiogenesis and invasion by combined treatments directed against vascular endothelial growth factor receptor-2, epidermal growth factor receptor, and vascular endothelial-cadherin, *Clin. Cancer Res.* 11 (2005) 4934–4940.
- [30] Y.C. Yung, S. Cheshier, J.G. Santarelli, Z. Huang, A. Wagers, I. Weissman, V. Tse, Incorporation of naive bone marrow derived cells into the vascular architecture of brain tumor, *Microcirculation* 11 (2004) 699–708.
- [31] R.K. Jain, Molecular regulation of vessel maturation, *Nat. Med.* 9 (2003) 685–693.
- [32] F.A. Eskens, J. Verweij, The clinical toxicity profile of vascular endothelial growth factor (VEGF) and vascular endothelial growth factor receptor (VEGFR) targeting angiogenesis inhibitors; a review, *Eur. J. Cancer* 42 (2006) 3127–3139.
- [33] T. Kamba, D.M. McDonald, Mechanisms of adverse effects of anti-VEGF therapy for cancer, *Br. J. Cancer* 96 (2007) 1788–1795.
- [34] N.A. Peters, D.J. Richel, J.J. Verhoeff, L.J. Stalpers, Bowel perforation after radiotherapy in a patient receiving sorafenib, *J. Clin. Oncol.* 26 (2008) 2405–2406.
- [35] J. Dietrich, A.D. Norden, P.Y. Wen, Emerging antiangiogenic treatments for gliomas – efficacy and safety issues, *Curr. Opin. Neurol.* 21 (2008) 736–744.
- [36] K.J. Williams, B.A. Telfer, S. Brave, J. Kendrew, L. Whittaker, I.J. Stratford, S.R. Wedge, ZD6474, a potent inhibitor of vascular endothelial growth factor signaling, combined with radiotherapy: schedule-dependent enhancement of antitumor activity, *Clin. Cancer Res.* 10 (2004) 8587–8593.
- [37] S. Ning, D. Laird, J.M. Cherrington, S.J. Knox, The antiangiogenic agents SU5416 and SU6668 increase the antitumor effects of fractionated irradiation, *Radiat. Res.* 157 (2002) 45–51.
- [38] M.L. Veronese, A. Mosenkis, K.T. Flaherty, M. Gallagher, J.P. Stevenson, R.R. Townsend, P.J. O'Dwyer, Mechanisms of hypertension associated with BAY 43–9006, *J. Clin. Oncol.* 24 (2006) 1363–1369.
- [39] J. Goldman, J.M. Rutkowski, J.D. Shields, M.C. Pasquier, Y. Cui, H.G. Schmokel, S. Willey, D.J. Hicklin, B. Pytowski, M.A. Swartz, Cooperative and redundant roles of VEGFR-2 and VEGFR-3 signaling in adult lymphangiogenesis, *FASEB J.* 21 (2007) 1003–1012.
- [40] I. Fischer, C.H. Cunliffe, R.J. Bollo, S. Raza, D. Monoky, L. Chiriboga, E.C. Parker, J.G. Golfinos, P.J. Kelly, E.A. Knopp, M.L. Gruber, D. Zagzag, A. Narayana, High-grade glioma before and after treatment with radiation and avastin: initial observations, *Neuro Oncol.* 10 (2008) 700–708.
- [41] J.L. Rubenstein, J. Kim, T. Ozawa, M. Zhang, M. Westphal, D.F. Deen, M.A. Shuman, Anti-VEGF antibody treatment of glioblastoma prolongs survival but results in increased vascular cooption, *Neoplasia* 2 (2000) 306–314.
- [42] K. Lamszus, P. Kunkel, M. Westphal, Invasion as limitation to anti-angiogenic glioma therapy, *Acta Neurochir. (Suppl.)* (2003) 169–177.
- [43] T. Martens, Y. Laabs, H.S. Gunther, D. Kemming, Z. Zhu, L. Witte, C. Hagel, M. Westphal, K. Lamszus, Inhibition of glioblastoma growth in a highly invasive nude mouse model can be achieved by targeting epidermal growth factor receptor but not vascular endothelial growth factor receptor-2, *Clin. Cancer Res.* 14 (2008) 5447–5458.

# Supplemental data

Table S1			
Mouse	Gastro intestinal tract	Ascites	Other
1	Omentum inflamed, pale liver	+	Enlarged lymph nodes
2(n)	Lymphomatous lesions jejunum, pancreatitis	-	Sinusitis Lymphomatous cells in lungs, lymphoma
3	Angitis in mesentery	-	-
4	-	-	Inflammatory lesions in nasal cavity, enlarged sup. cervical lymph nodes
Mouse	Gastro intestinal tract	Ascites	Other
5	-	++	-
6	Dilated lymph vessels, edematous changes, cecum dilation, edematous pancreas	++	Congestion, dark lungs, dilated blood vessels in bone marrow of skull bone
7	Edematous submucosa cecum, edematous pancreas	+	Inflammatory lesions nasal cavity, no bone marrow cells in skull bone
8	Dilated cecum, rigid colon: colitis	-	Lung angitis
9(n)	Edematous submucosa cecum and colon, edematous pancreas	++	-
10(n)	-	-	-
11(n)	Mild ileitis: infiltration in mucosa ileum	-	Degeneration of local nephrons
12	Amyloid-like deposit villi ileum, large cecum, focal liver necrosis	-	-
13	Mesenteric lymph node enlargement	-	Congestion
14	Mild inflammatory liver parenchyma	-	Interstitial pneumonia

Table S1: Pathology of mice treated with DC101 and irradiation. Mice 1-4 were sacrificed after 17 days of treatment. Mice 5-14 were sacrificed after 6 weeks of treatment. Mouse 2, 9, 10, 11 did not bear a tumor. -, Absence of pathology